Published online 25 September 2013 *Nucleic Acids Research, 2014, Vol. 42, No. 1* ***181–192***
doi:10.1093/nar/gkt863

macroH2A1 histone variant represses rDNA transcription

Rong Cong[1], Sadhan Das[1], Julien Douet[2], Jiemin Wong[3], Marcus Buschbeck[2], Fabien Mongelard[1,*] and Philippe Bouvet[1,*]

[1]Université de Lyon, Ecole Normale Supérieure de Lyon, CNRS USR 3010, Laboratoire Joliot-Curie, 69364 Lyon, France, [2]The Institute of Predictive and Personalized Medicine of Cancer (IMPPC), 08916 Badalona, Barcelona, Spain and [3]The Institute of Biomedical Sciences and School of Life Sciences, East China Normal University, Shanghai 200241, China

Received April 24, 2013; Revised August 30, 2013; Accepted September 4, 2013

ABSTRACT

The regulation of ribosomal DNA transcription is an important step for the control of cell growth. Epigenetic marks such as DNA methylation and posttranslational modifications of canonical histones have been involved in this regulation, but much less is known about the role of histone variants. In this work, we show that the histone variant macroH2A1 is present on the promoter of methylated rDNA genes. The inhibition of the expression of macroH2A1 in human HeLa and HepG2 cells and in a mouse ES cell line resulted in an up to 5-fold increase of pre-rRNA levels. This increased accumulation of pre-rRNA is accompanied by an increase of the loading of RNA polymerase I and UBF on the rDNA without any changes in the number of active rDNA genes. The inhibition of RNA polymerase I transcription by actinomycin D or by knocking down nucleolin, induces the recruitment of macroH2A1 on the rDNA and the relocalization of macroH2A1 in the nucleolus. Interestingly, the inhibition of rDNA transcription induced by nucleolin depletion is alleviated by the inactivation of macroH2A1. These results demonstrate that macroH2A1 is a new factor involved in the regulation of rDNA transcription.

INTRODUCTION

Ribosome biogenesis is of utmost importance to cell proliferation; it uses large amounts of cellular resources to produce >150 ribosomes per second in proliferating mammalian cells. This endeavour draws on many concerted cellular processes that converge to a central hub, the nucleoli. As such, nucleoli host the major events of the phenomenon, among which is the transcription of rRNA-encoding genes by the RNA polymerase I (RNAPI). RNAPI activity may represent up to 35% of total transcription in dividing mammalian cells (1). In human, this is made possible by the existence of ~300–400 rDNA gene copies per haploid genome, distributed on five clusters on chromosomes 13, 14, 15, 21 and 22 (2,3). Each cluster consists of repeated alternations between a gene (an ~14-kb coding region and its associated regulatory sequences), and an ~30-kb intergenic spacer (IGS). RNAPI transcription produces a large pre-rRNA 47S precursor that is processed and yields a copy of each of the mature 18S, 5.8S and 28S rRNA.

Numerous pathways regulate RNAPI activity, some acting through epigenetic modifications. In many dividing cells, including mammalian cells, only a fraction of the rDNA gene copies is active, while the others are kept silenced. Inactive copies may be characterized by different epigenetic features (4,5). These include methylated CpG dimers, tri-methylated H4K20 and tri-methylated H3K27. Conversely, active copies display H4K12 acetylation, H3K4 tri-methylation and unmethylated CpGs. Antagonistic molecular complexes establish these different marks. Among them, the nucleolar remodelling complex (NoRC) is a repressive chromatin remodeling complex that contains the SNF2h ATPase and TIP5 which, through its interaction with transcription termination factor-1 (TTF-1), brings NoRC to the promoter and, in turn, recruits chromatin-modifying activities, including DNA methyltransferase, histone methyltransferase and histone deacetylase such as HDAC1. On active rDNA promoters TTF1 also recruits the multifunctional Cockayne Syndrome group B protein (CSB) to the rDNA promoter (6). A complex formed by CSB, which is a chromatin remodeler and a DNA-dependent ATPase itself, and G9a, a histone H3 K9 methyltransferase, plays an important role in the activation of transcription. H3K9 di-methylation can be found on both CpG methylated and

*To whom correspondence should be addressed. Tel/Fax: +33 4 72 72 8016; Email: pbouvet@ens-lyon.fr
Correspondence may also be addressed to Fabien Mongelard. Tel/Fax: +33 4 72 72 8016; Email: fabien.mongelard@ens-lyon.fr

unmethylated rDNA (4). Since only a fraction of unmethylated rDNA is transcriptionally active (7), the role of H3K9 di-methylation in transcriptional activation remains unclear. The mechanisms that decide on the recruitment of NoRC versus CSB and thus determine the transcriptional state of the rDNA cluster, remain to be determined.

In this already complex picture, and beyond the identification of key players, recent results also strengthened the idea that complexity of rDNA transcription regulation through chromatin transactions cannot be summed up just in terms of On and Off bistable epigenetic states (4,5). Intermediate states do exist, whose existence seems to depend on the action of other complexes such as CHD4/NurD. Action of this complex is believed to promote the establishment of a poised state of rDNA gene, i.e. nontranscribed but permissive to transcriptional activation, in which preinitiation complexes are present on promoters whose DNA is unmethylated while histones carry both heterochromatin and euchromatin marks (8). Along these lines, we have recently shown that nucleolin, one of the most abundant nucleolar proteins, plays a positive role in RNAPI transcription without affecting the number of active copies (9). Nucleolin inhibits the binding of TTF1 to the promoter and reduces the recruitment of TIP5 and HDAC1, ultimately counteracting the establishment of heterochromatin marks and promoting rDNA transcription.

Beside posttranslational modifications of canonical histones, incorporation of histone variants plays a less-recognized role in rDNA regulation. Recently, the histone H2A variant macroH2A has been identified as modulator of rDNA transcription during seasonal acclimatization of carp fish (10), although little is known about the mechanisms involved. MacroH2A isoforms are structurally unique, possessing a 30-kDa nonhistone macrodomain at the C-terminus [reviewed by (11)]. Two distinct genes encode macroH2A1 and macroH2A2, the former being expressed in the form of two splice variants (macroH2A1.1 and macroH2A1.2). Their role in RNAPII transcription has proven to be complex and context-dependent. While they are generally thought to be part of repressive chromatin domains, induction of some genes requires the presence of macroH2A1 (12–14). Interestingly, nucleolin can act as a co-remodeler on macroH2A1 containing chromatin templates (15). These facts have prompted us to study the function of macroH2A1 in RNAPI transcription. In this article, we show that macroH2A1 is present on rDNA where it exerts a repressive effect on transcription.

MATERIALS AND METHODS

Cell lines and siRNA transfection

HeLa and HepG2 cells were cultured in Dulbecco's modified Eagle medium (DMEM, Gibco) supplemented with 10% fetal bovine serum (FBS) (Gibco) at 37°C in 5% CO_2. HeLa cells (6×10^5) were transfected with siRNA (Eurogentec) using Lipofectamine 2000 (Invitrogen) as described previously (16). The siRNA sequences used are listed in Supplementary Table S1. The mouse ES cell line E14 was maintained in minimal essential medium (Sigma) supplemented with 20% FBS (Hyclone), 1% penicillin-streptomycin, 1% glutamax, 1% nonessential amino acids, 1% sodium pyruvate and 0.2% ß-mercaptoethanol, in the presence of leukemia inhibitory factor corresponding to 1000 U/ml. For the induction of differentiation, 1 μM retinoic acid was added directly to the plates in LIF-free medium. HepG2 and mouse embryonic stem (mES) cells were transduced with retro- and lentiviral macroH2A-specific shRNA cassettes as described (12,17). Cells were harvested 96 h after transfection or puromycin-selection, and proteins and RNAs were analyzed by western blot and RT-QPCR, respectively. For the inhibition of RNAPI transcription, cells were treated for 3 h with actinomycin D (AMD; 5 μg/ml, Sigma) diluted in DMEM with 10% FBS.

Transcription analysis by RT-QPCR

Total RNA was prepared by TRIzol (Invitrogen) extraction and digested with 20 U of RNase-free DNase I (Roche Diagnostics) for 1 h at 37°C. One hundred nanograms of total RNA were reverse-transcribed using random hexamer primers and first strand cDNA synthesis kit (Fermentas) and the synthesized cDNA was used for RT-QPCR using FastStart Universal SYBR Green Master (ROX) (Roche). Primer sequences used are listed in Supplementary Table S2.

Immunofluorescence

HeLa cells grown on glass coverslips were washed with phosphate buffered saline (PBS), fixed with 4% paraformaldehyde in PBS for 10 min at room temperature, washed three times with PBS and fixed with −20°C methanol on ice for 20 min, then washed three times with PBS and permeabilized with 0.1% Triton X-100 in PBS for 2×5 min at room temperature. After two washes in PBS, nonspecific binding of antibodies was blocked with 10% fetal calf serum in PBS. After three washes with PBS, coverslips were incubated with primary antibodies at 37°C for 1 h. After two washes in PBS with 0.1% Triton X-100, coverslips were incubated with secondary antibodies coupled with Alexa dyes (A555 or A647). After two more washes in PBS with 0.1% Triton X-100, the coverslips were washed in PBS, rinsed in ddH_2O and briefly dipped in 100% ethanol. After a quick dry, cover slips were mounted with Fluoromount G containing 200 ng/ml DAPI.

Chromatin immunoprecipitation and DNA methylation assays

Chromatin immunoprecipitation (ChIP) assays were done as described earlier (18). HeLa cells were cross-linked for 10 min with 1% formaldehyde in the culture medium at room temperature. Glycine (0.125 M) was added, and the cells were rocked for 5 min to stop the reaction. The cells were suspended in 200 μl of sodium dodecyl sulfate (SDS) lysis buffer (1% SDS, 10 mM EDTA, 50 mM Tris, pH 8.1), and sonication was performed to produce DNA fragments of 200–1000 bp in length. Chromatin was diluted

10-fold with ChIP dilution buffer (0.01% SDS, 1.1% Triton X-100, 1.2 mM EDTA, 16.7 mM Tris, pH8.1, 167 mM NaCl), precleared and immunoprecipitated with the respective antibodies. Precipitated DNA and protein complexes were reverse cross-linked and purified through phenol/chloroform extraction and ethanol precipitation.

The purified DNAs were amplified by real-time polymerase chain reaction (PCR) using StepOne Plus (Applied Biosystems) and FastStart Universal SYBR Green Master (ROX) (Roche). Primers for real-time PCR were designed or as reported (19) and listed in Supplementary Table S2.

To monitor CpG methylation of rDNA at −9 (20), DNA was digested with 20 U of HpaII or MspI, or it was mock-digested. For quantification, the digested DNA along with an equal amount of the mock-digested DNA were amplified by real-time PCR using the H42.9 primer pair (see Supplementary Table S2) that flanks the −9 HpaII/MspI site on the human rDNA promoter region (19). The relative resistance to HpaII digestion was calculated by normalizing the amount of DNA resistant to HpaII to that of mock-digested DNA.

Psoralen cross-linking and Southern blot

HeLa cells grown in 60-mm Petri dishes (0.8×10^6 cells/Petri) were placed in serum-free medium (1.5 ml) just before cross-linking began. A 1/20 volume (75 µl) of 200 µg/ml trioxsalen (4,5′,8-trimethylpsoralen, Sigma) in methanol was added with gentle mixing, and after 5-min incubation, cells were irradiated on ice for 5 min with a 366-nm ultraviolet lamp (BlackRay model B-100 A, 100 W) placed at a distance of 6–7 cm. Cross-linking was repeated three more times, each time adding fresh trioxsalen. Subsequently, the cells were washed with PBS and lysed with 0.5 ml of lysis buffer (10 mM Tris, pH 7.5, 50 mM NaCl, 25 mM EDTA, 2% SDS). Proteinase K (1 mg/ml, Fermentas) was added, and the combined lysate was incubated overnight at 50°C, adding fresh proteinase K after the first 2 h. The genomic DNA was then deproteinized twice with phenol/chloroform, ethanol precipitated and resuspended in 250 µl of TE, pH 7.5, and 0.1% SDS. Twenty micrograms of RNAse A (Fermentas) was added and after 30 min at 37°C, 0.5 mg/ml Proteinase K was also added and incubation continued for another 1 h at 50°C. After two phenol/chloroform extractions, the genomic DNA was ethanol precipitated, resuspended in 50 µl of TE and quantified. About 10 µg of genomic DNA was digested overnight with BamHI and resolved on a 1% TAE agarose gel at $2\,V.cm^{-1}$ for 22 h in the absence of ethidium bromide. The gel was subsequently ethidium bromide-stained, photographed, its cross-links reversed by ultraviolet irradiation at 254 nm ($4000\,mJ \cdot cm^{-2}$) in a Stratalinker 1800 cross-linker (Agilent Technologies) and transferred onto a Biodyne B membrane (Pall). Hybridization was performed overnight at 65°C with labeled DNA probes in Southern Church Buffer (0.5 M sodium phosphate, pH 7.2, 1 mM EDTA, pH8.0, 7% SDS, 1% bovine serum albumin). Subsequently, membranes were washed with 6×saline sodium citrate (SSC), 2× SSC and 0.1× SSC and 0.1% SDS. Data were collected using a FujiFilm FLA-5100 analyzer and analyzed with MultiGauge software.

Metabolic labeling and analysis of pre-rRNA transcription and processing

Cells (4×10^5) were incubated at 37°C in 3 ml of DMEM without phosphate (Invitrogen) supplemented with 10% fetal calf serum, 25 mM Hepes (Invitrogen). After 2 h, [^{32}P]Pi (GE Healthcare) was added to the medium (125 µCi/ml) for 3 h. At the end of the labeling, cells were centrifuged for 5 min at 300*g* and total RNA was extracted with RNeasy kit (Qiagen), separated by denaturing electrophoresis and the gel was dried before exposure. The RNA corresponding to an equal number of cells was loaded for each sample. Data were collected and analyzed as described above.

Antibodies

The following antibodies were used: A rabbit polyclonal antibody against human nucleolin (number 5567; developed by our laboratory), anti-histone macroH2A1 (07–219, Upstate), anti-histone H3 (C-terminal, Upstate), anti-nucleolin monoclonal antibody (KAM-CP100, Stressgen), anti-B23 antibody (ab10530, Abcam), anti-RPA116 (a generous gift from Ingrid Grummt) and anti-UBF (F-9) (sc-13125; Santa Cruz).

RESULTS

MacroH2A1 is associated with methylated rDNA

ChIP was performed to identify macroH2A1-associated loci using PCR primers designed inside the human rDNA gene (Figure 1A). As seen in Figure 1B, macroH2A1 is detected all along the rDNA unit, though to different extent. It is most abundant in the promoter region (UCE, CORE), and present at basal levels throughout the rest of the region. Histone H3 distribution along the rDNA repeat is homogenous (Supplementary Figure S1A), and therefore the normalization of macroH2A1 distribution with histone H3 occupancy does not change the distribution pattern of macroH2A1 (Supplementary Figure S1B).

In eukaryotic cells, rDNA copies exist in either transcriptional active or inactive state (5). The DNA methylation status of the promoter can be analyzed to distinguish silent copies, which are methylated and unsensitive to HpaII digestion, from transcriptional competent and active copies, which display opposite characteristics (18). To assess a potential preferential association of macroH2A1 with one of these subsets, a ChIP-chop experiment was carried out, in which DNA pulled down in ChIP assays with anti-macroH2A1 antibody was digested with HpaII before PCR amplification, and the level of methylated rDNA (HpaII resistant) at position −9 was determined. Methylation at this CpG site was previously shown to be associated with rRNA promoter repression (20). We found that in HeLa cells, ∼50% of rDNA genes are methylated at −9 CpG. macroH2A1 is preferentially

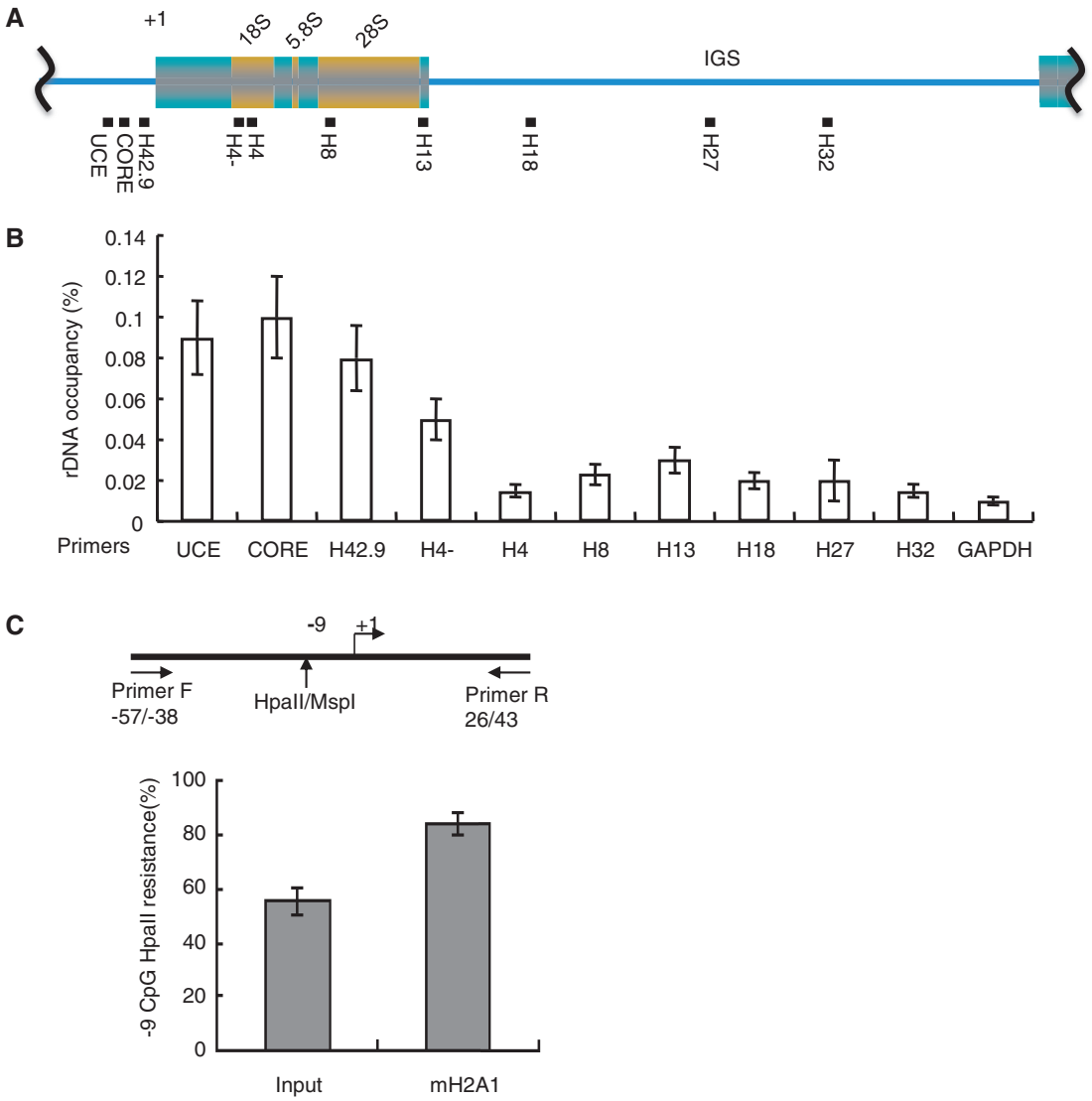

Figure 1. macroH2A1 is associated with methylated rDNA. (**A**) Schematic representation of a human rDNA repeat. The positions of QPCR amplicons in ChIP assays are indicated with solid bars. (**B**) ChIP-QPCR analysis of the enrichment of macroH2A1 on rDNA. Cross-linked chromatin from HeLa cells was immunoprecipitated with the macroH2A1 antibody, DNA was analyzed by QPCR using sets of primers indicated in Panel A. The percentage of DNA immunoprecipitated with anti-macroH2A1 antibody was calculated relative to the ChIP input DNA. Values are means ± SD derived from three independent ChIP experiments, each tested by at least three independent QPCR reactions. (**C**) macroH2A1 is associated with methylated rDNA repeats. ChIP input DNA and DNA precipitated by macroH2A1 antibody were digested with HpaII or MspI, respectively, or they were mock-digested. The relative levels of HpaII-resistant methylated rDNA copies (gray bars) were determined by QPCR with the pair of primers that flanks the HpaII/MspI site on the rDNA promoter as indicated after normalization to mock-digested DNA.

associated with genes that are methylated at this site (~85%) (Figure 1C), suggesting a role for macroH2A1 in the repression of rDNA copies.

macroH2A1 is required for the repression of rDNA transcription

To assess the potential involvement of macroH2A1 in repressing rDNA, the steady state pre-rRNA level was measured in HeLa cells depleted in macroH2A1. On siRNA treatment, macroH2A1 levels were efficiently reduced as seen by western blot, immunofluorescence and RT-QPCR (Figure 2A–C). Under these conditions, a 3.5-fold increase in the relative amount of 47 S pre-rRNA was observed (Figure 2C). In metabolic labeling experiments (Supplementary Figure S2), we observed in macroH2A1-depleted cells a 1.5 increase of the incorporation of labeled nucleotides in matured rRNA species. The stressful conditions of this *in vivo* labeling experiment (incubation of the cells before labeling in phosphate-free medium), and the labeling period that may be insufficient to reach steady state labeling, may explain this smaller increase of ribosomal RNA in macroH2A1-depleted cells compared with the RT-QPCR data. However, both metabolic labeling and RT-QPCR indicate a significant and reproducible increase in rRNA production. Importantly, normal processing of the transcripts was maintained in macroH2A1-depleted cells (Supplementary Figure S2B and C), indicating that no gross defect in transcript maturation

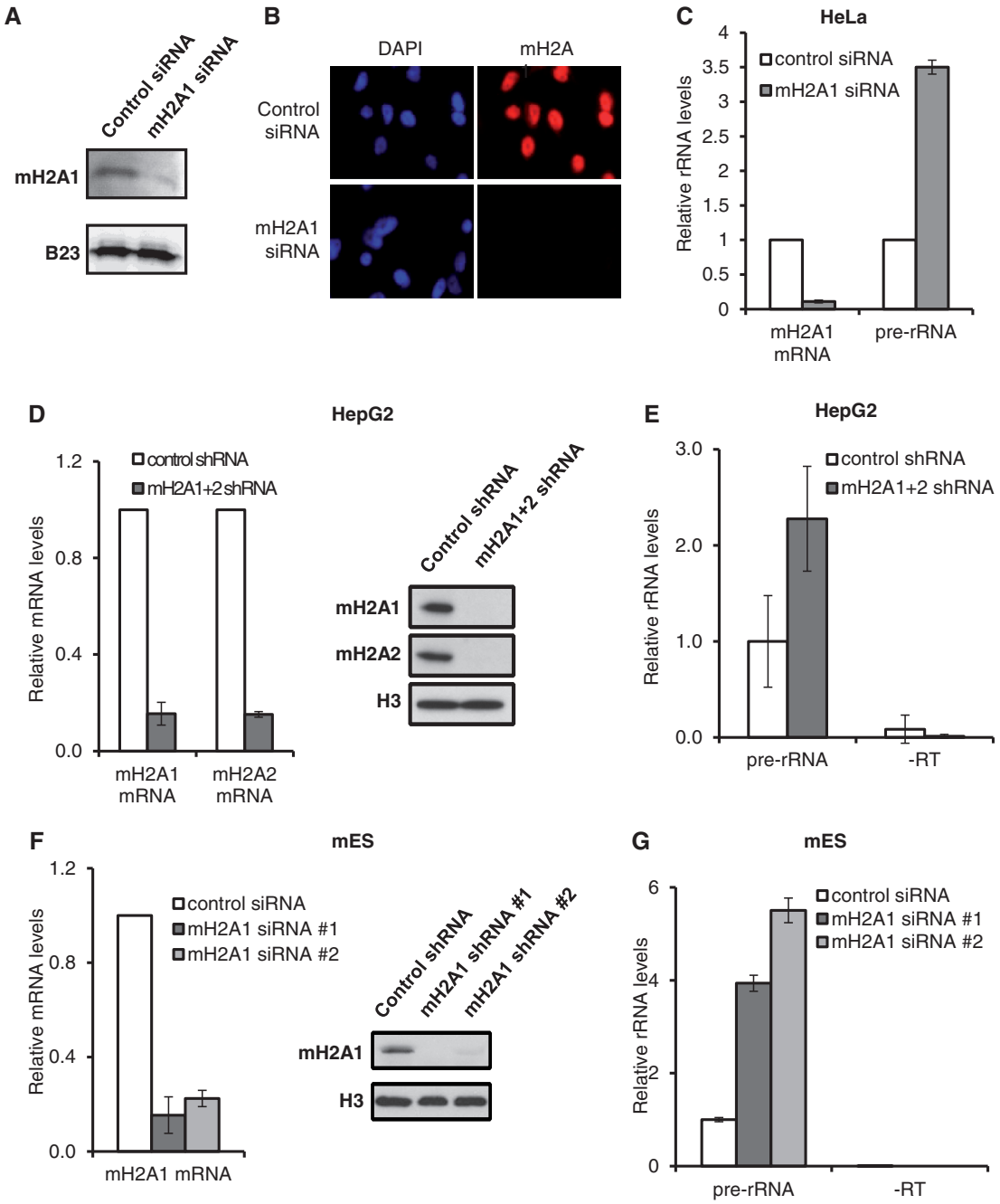

Figure 2. macroH2A1 represses Pol I transcription. (**A**) Western Blots of macroH2A1 in HeLa cells transfected with control or macroH2A1 siRNA. B23 antibody was used as a control. (**B**) Immunofluorescence using anti-macroH2A1 antibody (red) in HeLa cells transfected with control or macroH2A1 siRNA. DNA was stained with DAPI in blue. The bar represents 10 μm. (**C**) Depletion of macroH2A1 increases rRNA transcription. Total RNA was extracted 3 days after transfection of HeLa cells with control or macroH2A1 siRNA and used for RT-QPCR. Data were normalized to the amount of β-actin mRNA and to the amount of pre-rRNA in control cells. Data are from three independent experiments. (**D**) RT-qPCR and western blot showing the depletion of macroH2A1 and 2 at the RNA and protein levels in HepG2 cells by transduction of retroviral shRNA cassettes specific for macroH2A (sh mH2A1+2) or controls (sh Scr). For the RT-QPCR, data were normalized with the expression of two different housekeeping genes GAPDH and HPRT. For the western blot, immune-detection of histone H3 ensures equivalent amounts of protein were loaded. (**E**) Depletion of macroH2A1 increases rRNA accumulation in HepG2. Total RNA was extracted from control or macroH2A1+2-depleted cells. Negative controls were performed without reverse transcriptase (-RT). Data from three independent experiments were normalized to the average amount of mRNA of two housekeeping genes (GAPDH and HPRT). (**F**) RT-QPCR and western blot showing the depletion of macroH2A1 the RNA and protein levels in mES cells by transduction of two different lentiviral shRNA cassettes (sh mH2A1 #1 and #2). For the RT-QPCR, data were normalized to the average amount of mRNA of two housekeeping genes. For the western blot, immune-detection of histone H3 ensures equivalent amounts of protein were loaded. (**G**) Depletion of macroH2A1 increases rRNA transcription under self-renewal conditions. Total RNA from three independent biological replicates were extracted for control (sh Scr) or macroH2A1-depleted cells (sh mH2A1 #1 and #2). Negative controls were performed without reverse transcriptase (-RT).

are induced by a shortage in macroH2A1, whose role seems therefore to be linked solely to transcription.

The control exerted by macroH2A1 on rDNA is conserved in different cell types as shown Figure 2D–F. Knocking down macroH2A1 and macroH2A2 in the human hepatocarcinoma cell line HepG2 (Figure 2D) leads to a 2-fold accumulation of rDNA transcripts (Figure 2E). The largest effect was observed by depleting macroH2A1 in mES cells. Mouse ES cells predominantly express macroH2A1.2 (12), and knocking down macroH2A1 transcripts with two different shRNAs (Figure 2F) induces a 5-fold increase of rDNA transcripts (Figure 2G) when cells were grown under self-renewal conditions. Since expression of rDNA genes is coupled to cell growth rates, we analyzed the effect of macroH2A1 depletion on the cell cycle (Supplementary Figure S3). As previously found in mES cells (12), macroH2A1 depletion does not affect the proportion of cells in various phases of the cell cycle, and therefore it is unlikely that the increased rDNA expression would be the consequence of an indirect effect of macroH2A1 on the cell growth.

Transcription of rDNA can be modulated through the control of the initiation or elongation rates at each repeat unit. It can also be epigenetically controlled by reducing or increasing the number of active gene copies. To identify the contribution of macroH2A1 to each phenomenon, we first examined the effect of macroH2A1 knockdown on the relative proportion of active and inactive rRNA genes using psoralen, a DNA cross-linking reagent. Active rRNA genes, associated with nascent rRNA transcripts, have an open chromatin structure that is accessible to psoralen (21). Conversely, silent genes are inaccessible to psoralen. After psoralen cross-linking, the active and inactive rRNA genes can be distinguished by Southern blotting, thanks to their different rates of migration (21,22). We found no significant difference in the percentage of active genes between the control and macroH2A1-depleted cells (Figure 3A), which is ~20% in HeLa cells in agreement with the data of previous work using this psoralen technique in human cells (7). In a positive control experiment, psoralen analysis demonstrated a significant reduction in the number of active rRNA genes after UBF sirRNA knockdown. We next analyzed the methylation state of the rDNA promoter at the −9 CpG sites as described in Figure 1C. In macroH2A1-depleted cells, the level of methylated (HpaII resistant) rDNA at −9 CpG does not change (Figure 3B), which is in good agreement with the absence of a change in the ratio of the active-inactive copies observed in the psoralen cross-linking experiment. These results show that macroH2A1 is not required for the maintenance of closed chromatin conformation at the rDNA loci. It also suggests that the increased accumulation of rRNA seen on macroH2A1 depletion is not mediated by the activation of additional rRNA gene copies, but rather by the increased transcription of active units.

To identify the chromatin posttranslational modifications that may be linked to the enhanced rDNA transcription, ChIP experiments using antibodies directed against H3K4me3, H3K9me2 and H4K12Ac were performed to analyze the rDNA promoter region (H42.9, see Figures 1A and 3C). The knockdown of macroH2A1 leads to the increase of the transcriptional active markers H3K4me3 and H4K12Ac on the rDNA promoter. This is in support of the fact that macroH2A1 depletion results in an increase of pre-rRNA levels. H3K9me2 level on rDNA promoter is also increased on macroH2A1 depletion. Although H3K9me2 is usually considered as a repressive mark, it could be found on both CpG methylated and unmethylated sites on rDNA, suggesting that it could be also associated to active rDNA gene copies (6). However, only a fraction of unmethylated rDNA is transcriptionally active (7).

To get additional insight into the cause of the elevated rRNA production after macroH2A1 removal, changes in the occupancy of RNAPI across the locus were measured using ChIP. Figure 4A shows that siRNA-induced removal of macroH2A1 is accompanied by a significantly increased recruitment of RNAPI throughout the coding sequence and in the promoter region. Together with the absence of change in the number of active gene copies, this result suggests that the increased accumulation of rRNA is due to an enhanced recruitment of RNAPI to the already active units.

The recruitment of RNAPI to the rDNA promoters is controlled by different factors among which is UBF. We thus measured the impact of macroH2A1 knockdown on the presence of UBF on rDNA. As seen in Figure 4B, at the UCE and CORE promoter regions, an almost 5- and 4-fold increase is measured, respectively. In the coding region, UBF association also increases, to different extent in different part of the gene. Surprisingly, more UBF is also detected under these conditions in the IGS. These data suggest that the presence of macroH2A1 is able to modulate the recruitment of UBF.

MacroH2A1 is relocalized to the nucleoli after nucleolin depletion

Nucleolin, a major nucleolar protein, displays histone chaperon and co-remodeling activity toward macroH2A1 (15); furthermore, nucleolin is required for normal rRNA transcription (16,23,24). Therefore, we determined whether macroH2A1 distribution and abundance along the rDNA repeat are somehow dependent on nucleolin (Figure 5). For that purpose, ChIP assays were carried out after siRNA-induced nucleolin knockdown. Strikingly, nucleolin depletion leads to a dramatic increase of macroH2A1 presence on different regions of the rDNA, including the promoter regions and coding regions and in the IGS (Figure 5A). This increased macroH2A1 load on rDNA is not the consequence of *de novo* synthesis of macroH2A1, as western blot analysis showed that the nucleolin knockdown does not impact levels of macroH2A1 (Figure 5B). Immunofluorescence staining of HeLa control and nucleolin-depleted cells show that macroH2A1 is present in nuclear structures that are labeled by fibrillarin (Figure 5C) identifying these structures as nucleoli. Therefore, the increased association of macroH2A1 with rDNA is most likely the consequence of a relocalization of the protein. We previously showed that on nucleolin depletion the level of methylation at the −9 CpG site is not

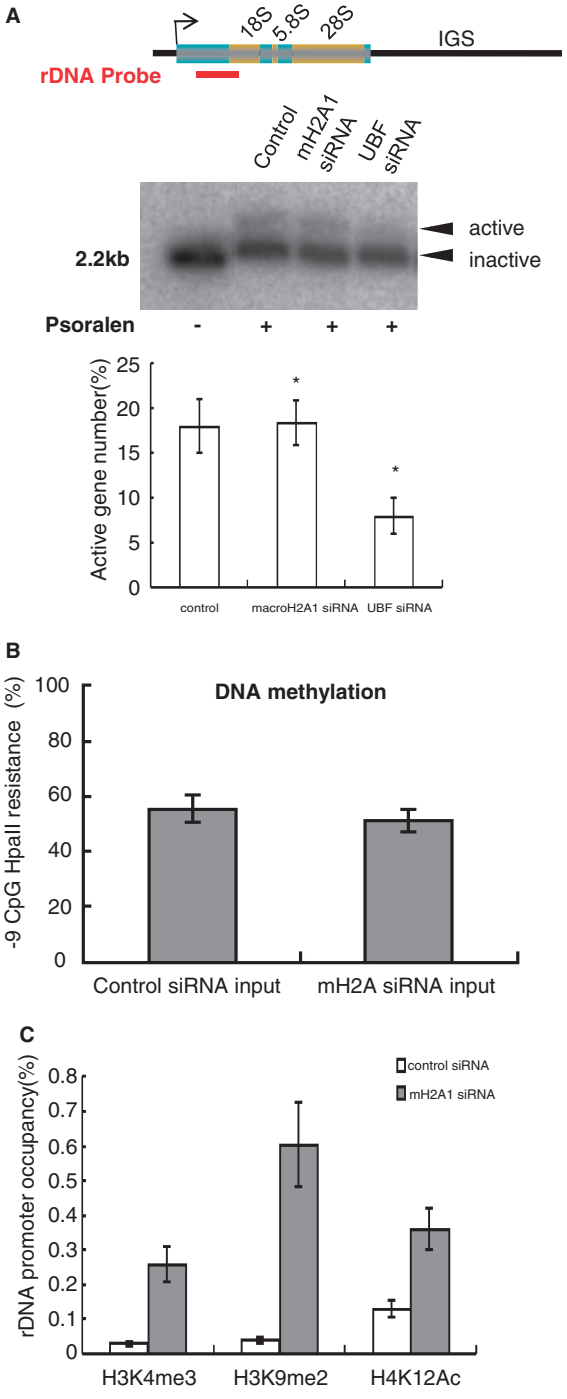

Figure 3. macroH2A1 does not affect the number of active gene number and rDNA methylation, but affects epigenetic marks on rDNA. (**A**) Psoralen cross-linking analysis. Schematic representation of the human rDNA indicating the probe used in Southern blot (upper panel). A representative Southern blot is shown. The first lane (without psoralen) is the control showing the migration of the uncross-linked 2.2 kb fragment. The lower panel show the quantitative analysis of three independent experiments. Asterisk indicates that the difference is significant ($0.01 < P < 0.05$) compared with the control group analyzed by Student's *t*-test. (**B**) Depletion of macroH2A1 does not change the level of methylation at the −9 CpG site. ChIP input DNA from control or macroH2A1 siRNA-treated HeLa cells was digested with HpaII or MspI, respectively, or they were mock-digested. The relative levels of HpaII-resistant methylated rDNA copies (gray bars) were determined by QPCR with the pair of primers that flanks the HpaII/MspI site on the rDNA promoter as indicated after normalization to mock-digested DNA. (**C**) Determination by ChIP of changes in posttranslational modifications of rDNA-associated histones after macroH2A1 siRNA-induced knockdown. QPCR was performed on the rDNA promoter using H42.9 pair of primers (see Figure 1A for localization and Supplementary Table S2 for primer sequences). Values are mean ± SD from three independent experiments.

changed (9). As macroH2A1 is preferentially associated with methylated rDNA genes (Figure 1C), we next checked if the enhanced recruitment of macroH2A1 on rDNA changed the proportion of methylated versus unmethylated genes bound to macroH2A1. In absence of nucleolin, this ratio is not changed (Figure 5D).

The enhanced deposition of macroH2A1 under nucleolin shortage may be indirectly due to reduced transcription, rather than to a direct role of nucleolin as a co-remodeler and histone chaperon toward macroH2A1. In an attempt to distinguish between these two possibilities, we inhibited RNAPI transcription by treating cells with AMD (Figure 6A), and determined the localization of macroH2A1 in these cells by immunofluorescence (Figure 6B). Interestingly, the drastic redistribution of macroH2A1 in the nucleoli induced by nucleolin was also observed on AMD treatment. A ChIP assay performed after AMD treatment confirmed the enhanced association of macroH2A1 all along the rDNA unit (Figure 6C). Taken together, these results suggest that nucleolin and active RNAPI transcription restrain the presence of macroH2A1 on the rDNA units.

rDNA repression by nucleolin depletion is alleviated by the inactivation of macroH2A1

To get a clearer view of the functional links between nucleolin and macroH2A1, expression of nucleolin or both proteins was suppressed in HeLa cells. As seen in Figure 7A, the siRNA-mediated knockdown efficiently reduces the targeted mRNAs. In the nucleolin knocked-down cell, pre-rRNA levels were severely reduced (Figure 7B), as we and others have already reported (9,16,23,24). Remarkably, in the double knocked-down cells, expression of pre-rRNA is restored to 80% of the control level. These results suggest that nucleolin and macroH2A1 act antagonistically, and that macroH2A1 is an important factor for the downregulation of rRNA expression when nucleolin expression is reduced.

DISCUSSION

The massive transcription of rDNA by RNAPI is under the control of sophisticated mechanisms that involve the immense complexity of chromatin structure and function. DNA methylation and histone posttranslational modifications have been identified as actors in these mechanisms. On the other hand, presence of histone variants in rDNA chromatin and their potential roles in the regulation of RNAPI activity have been reported in considerably less reports. Proteomic studies of the nucleolus (25,26) have

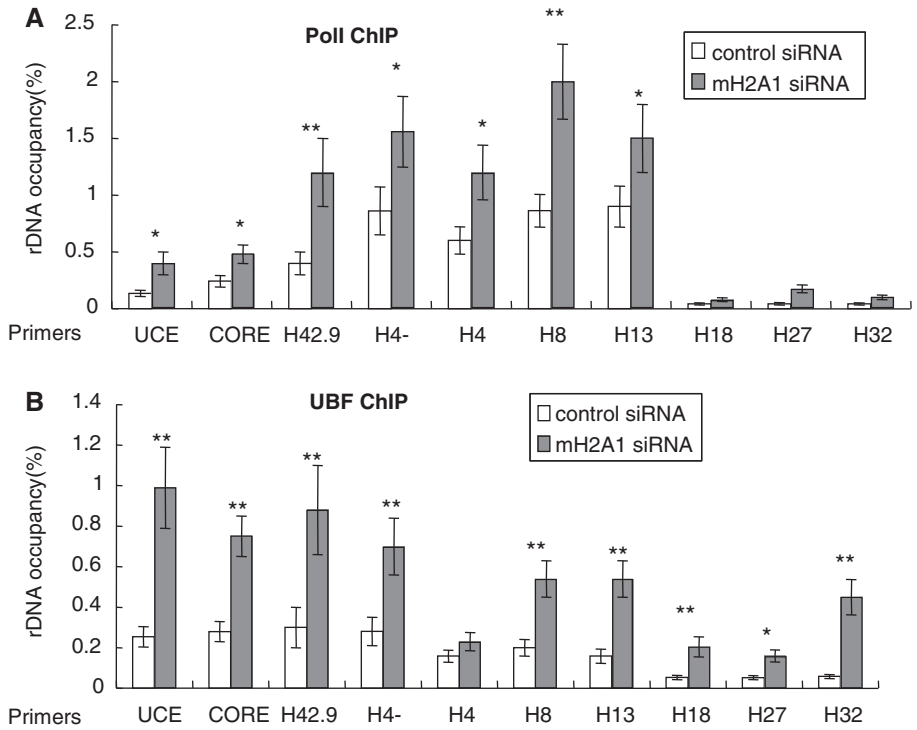

Figure 4. macroH2A1 depletion leads to the increase of the distribution of RNAPI and UBF on rDNA. (**A**) macroH2A1 depletion leads to an increase in UBF on rDNA. ChIP experiments with UBF antibody were performed in HeLa control and macroH2A1-depleted cells. The percentage of DNA immunoprecipitated with anti-UBF antibody was calculated relative to the ChIP input DNA. (**B**) macroH2A1 depletion increases the level of RNAPI on rDNA. ChIP experiments with RPA116 antibody were performed in HeLa control and macroH2A1-depleted cells. The percentage of DNA immunoprecipitated with anti-PRA116 antibody was calculated relative to the ChIP input DNA. Student's *t*-test was done between HeLa cells transfected with control siRNA and mH2A1 siRNA: *: $0.01 < P < 0.05$, **$P < 0.01$.

shown that the histone variant macroH2A1 is present in the nucleolus, and it has been suggested that this variant could be correlated with heterochromatic inactive copies of rRNA genes during seasonal acclimatization of the carp fish (10).

Using ChIP, we showed the presence of macroH2A1 on human rDNA (Figure 1B) and further found that its level varies along the repeat unit, being maximal in the promoter region, and relatively high at the end of the transcribed sequence. Conversely, it is low in the transcribed region, and that may be explained by the high histone exchange rate associated with intense transcription.The enrichment of macroH2A1 at the promoter (Figure 1B) is unlike patterns previously reported for RNAPII-transcribed genes (13,27). The preferential, but not exclusive, association of macroH2A1 with methylated promoters (Figure 1C) further suggests that it plays a role in repressing transcription, since this class of promoter is known to be repressed (5). siRNA-mediated knockdown of macroH2A1 resulted in an up to 5-fold increase of pre-rRNA levels (Figure 2). Such a strong effect of macroH2A1 in transcription regulation is not common, and the importance of macroH2A1 in the maintenance of an epigenetic state seems to depend on the context. MacroH2A1 appears dispensable for X inactivation (28) even if it is involved in the stability of the inactive X chromosome in MEFs (28). More generally, mouse lacking this histone can grow to adulthood (28,29), and in this respect, macroH2A1 seems to be part of silencing mechanisms that possess a high level of redundancy. For example, reactivation of Utx target genes during the iPS reprogramming of mouse wild-type fibroblast seems inhibited by the combination of macroH2A and H3K27me3 (28). On the other hand, macroH2A appears to be absolutely required to keep a mouse X chromosome inactive on transfer into a Xenopus oocyte (30). This latter situation is therefore reminiscent of the important repressive role of macroH2A1 that we observed on RNAPI transcription.

Interestingly, the activation we observed on macroH2A1 knockdown is not brought about by a measurable increase in the number of active rRNA genes, as indicated by a psoralen cross-link analysis (Figure 3A) or by a change of the methylation state of rDNA genes at the −9 CpG site (Figure 3B). These observations prompted us to assess potential changes in the loading of RNAPI. ChIP assays clearly showed that RNAPI abundance on rDNA significantly increased after macroH2A1 depletion, thus designating this histone variant as a regulator of RNAPI loading on the rDNA promoter or on transcription elongation (Figure 4A). This increase is seen together with an enhanced binding of UBF (Figure 4B). UBF is a key factor in the activation of RNAPI transcription, and may be in equilibrium with macroH2A1.

We have previously shown that the repression imposed by macroH2A1 on the remodeling of chromatin templates

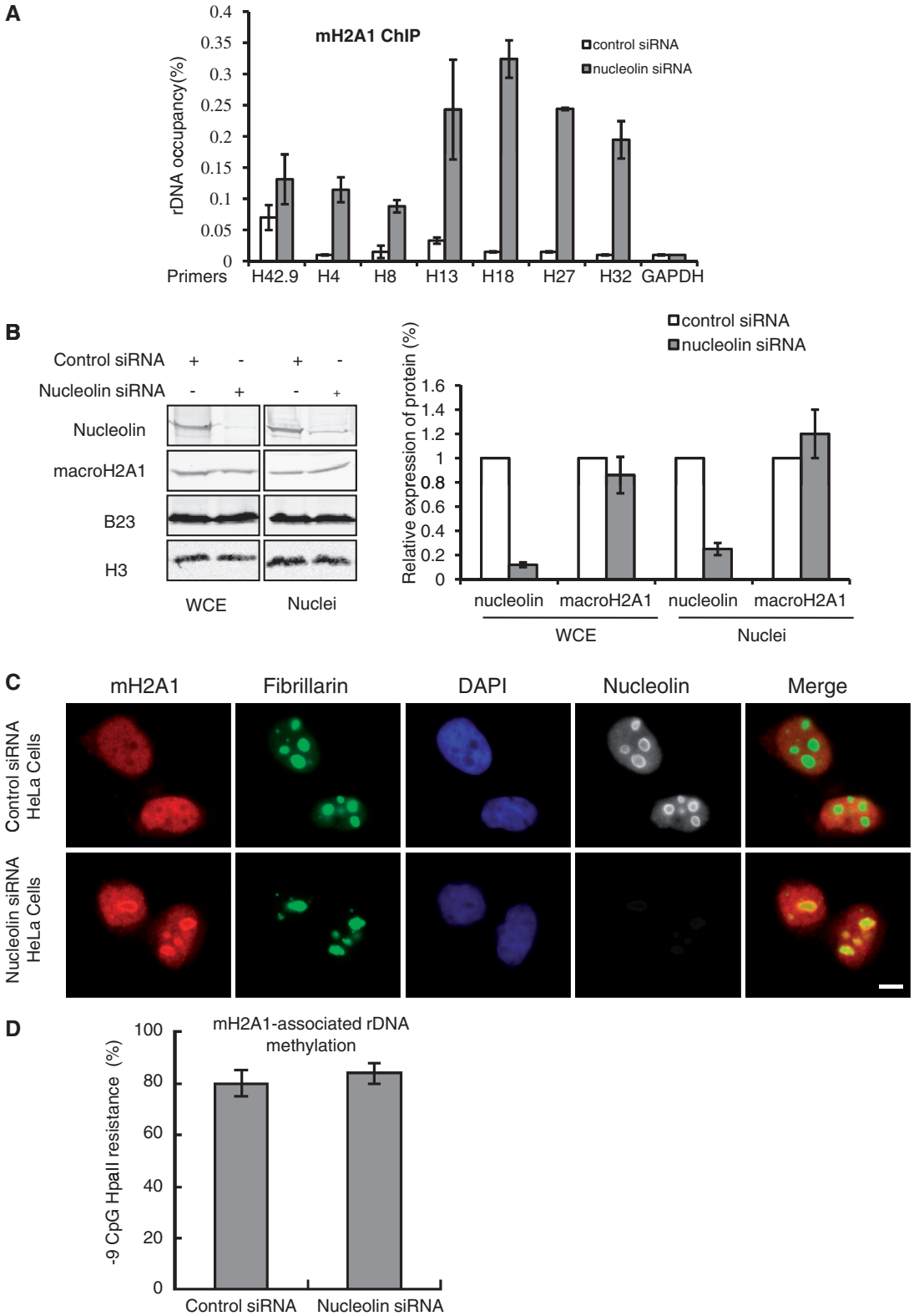

Figure 5. macroH2A1 is relocalized to the nucleoli after nucleolin depletion. (**A**) Nucleolin depletion increases the level of macroH2A1 all along the rDNA repeat. ChIP experiments with macroH2A1 antibody were performed in HeLa control and nucleolin-depleted cells. (**B**) Western blots showing the levels of macroH2A1, B23 and H3 in HeLa cells transfected with control or nucleolin siRNA. Whole cell extract (WCE) and nuclear extract (Nuclei) were analyzed 4 days after transfection. (**C**) Immunofluorescence studies of the localization of macroH2A1 (red), fibrillarin (green) and nucleolin (gray) in HeLa cells transfected with control or nucleolin siRNA. DNA was stained with DAPI. The bar represents 10 μm. (**D**) DNA precipitated by macroH2A1 antibody from control and nucleolin knockdown cells was digested with HpaII or MspI, or it was mock-digested. The relative levels of HpaII-resistant methylated rDNA copies (gray bars) were determined by QPCR with the pair of primers that flanks the HpaII/MspI site on the rDNA promoter as indicated after normalization to mock-digested DNA.

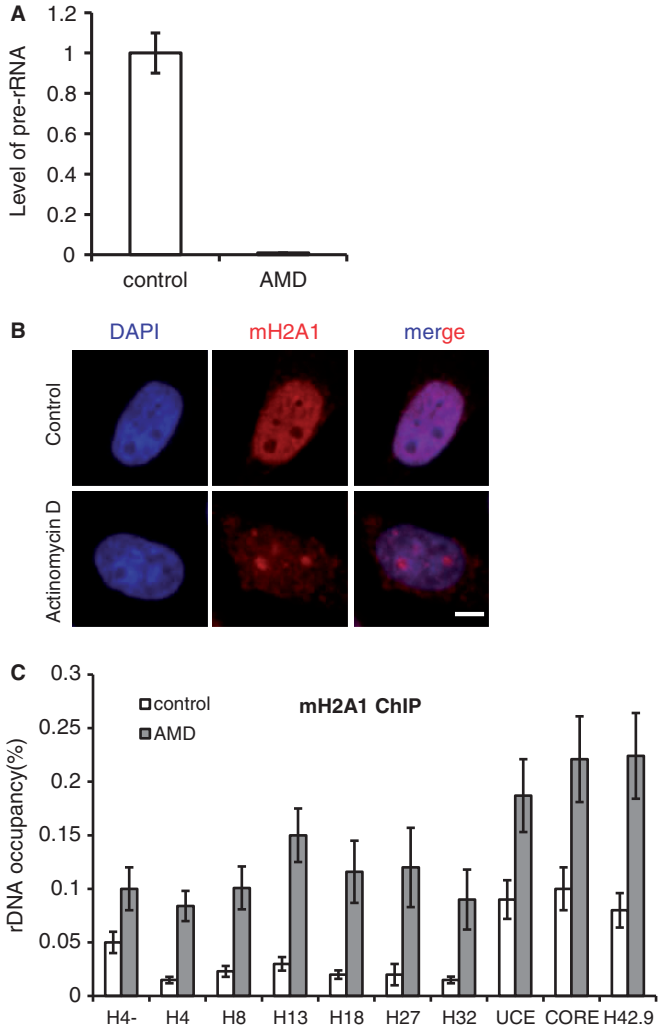

Figure 6. macroH2A1 is relocalized to the nucleoli after actinomycin treatment. (**A**) Inhibition of pre-rRNA transcription by AMD treatment. HeLa cells were treated with or without 5 µg/ml AMD for 3 h, then the level of pre-rRNA was monitored by RT-QPCR with the primers specific for 5′-ETS of human rDNA indicated in 'Materials and Methods' section. (**B**) Immunofluorescence of HeLa cells with macroH2A1 antibody treated with or without 5 µg/ml AMD for 3 h. DNA was stained with DAPI. The scale bar represents 10 µm. (**C**) AMD increases the level of macroH2A1 all along the rDNA repeat. ChIP experiments with macroH2A1 antibody were performed in HeLa cells treated with or without 5 µg/ml AMD for 3 h.

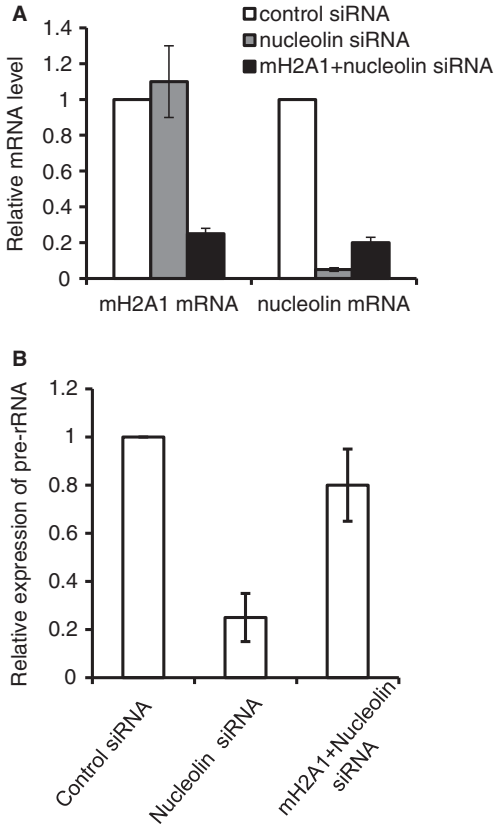

Figure 7. rDNA repression by nucleolin depletion is alleviated by the inactivation of macroH2A1. (**A** and **B**) The repression of rDNA transcription on nucleolin silencing was alleviated after the simultaneous inactivation of macroH2A1. HeLa cells were transfected with control, nucleolin or nucleolin and macroH2A1 siRNA, and total RNA was isolated and used for RT-QPCR. Data were normalized to the amount of β-actin mRNA and to the control cells. Data were from three independent experiments.

could be alleviated by nucleolin, which in this context acts as a co-remodeler and a histone chaperone (15). More recently, we described the importance of nucleolin in the maintenance of a heterochromatin state on rDNA, through the inhibition of the recruitment of TIP5 and HDAC1; nucleolin appears also to be required for optimal recruitment of UBF (9). The results reported in the present article therefore suggest that nucleolin and macroH2A1 may act antagonistically to epigenetically regulate rDNA transcription elongation, as shown in double knockdown experiments (Figure 7). The molecular mechanism linking nucleolin and macroH2A1 cannot be derived from our observations. We have recently shown that nucleolin knockdown has no measurable impact on rDNA methylation (9), and here we further show that nucleolin depletion does not result in an increased recruitment of macroH2A1 on methylated rDNA (Figure 5D). However, the chaperone and co-remodeling activities of nucleolin (15,31,32) might be implicated in the exclusion of macroH2A1 from rDNA genes. Nucleolin was shown to be capable of remodeling macroH2A1 nucleosomes that are otherwise resistant to remodeling machineries (15). This hypothesis is consistent with macroH2A1 accumulation in nucleoli and on rDNA genes after depletion of nucleolin, as seen by ChIP and immunofluorescence experiments (Figure 5), and with the increase of heterochromatin marks on rDNA genes that we have recently described on nucleolin depletion (9).

The gain of macroH2A1 after nucleolin depletion was more dramatic on the IGS than at the promoter and coding regions of rDNA (Figure 5A). How macroH2A1 is assembled on IGS in these conditions and whether this enrichment plays a role in the control of RNAPI transcription remain to be determined. It has been shown in the case of the inactive X chromosome that the noncoding RNA Xist plays an important role in macroH2A1 enrichment (33). rDNA silencing involves pRNA transcribed from IGS (34) and NoRC. It will be interesting to see

whether they are necessary for the recruitment of macroH2A1 in nucleolin-depleted cells.

Beside transcription, we also checked the potential role that macroH2A1 could play in the subsequent steps of processing and maturation of pre-rRNA. There is a close coordination between rRNA transcription, co-transcriptional processing and ribosome biogenesis (35). Stefanovsky *et al*. have proposed that such a concerted control of both elongation rate and transcript processing exists through changes in chromatin structure (36). In the case of some genes transcribed by RNAPII, another H2A variant, H2A.Bbd, is involved in the coupling of transcription and mRNA processing (37). Interestingly, in our observations, macroH2A1 does not seem to be required for the normal processing of pre-RNA, as no changes are seen after metabolic labeling of the transcripts on siRNA-mediated macroH2A1 depletion, thus arguing for a role of macroH2A1 limited to transcription.

SUPPLEMENTARY DATA

Supplementary Data are available at NAR Online.

ACKNOWLEDGEMENTS

The authors thank Vanesa Valero for technical assistance and T. Moss for advices to perform the psoralen experiment. They thank also PLATIM (PLAteau Technique d'Imagerie et de Microscopie, UMS3444, Lyon, FRANCE).

FUNDING

Agence Nationale de la Recherche [ANR- 07-BLAN-0062-01]; Région Rhône-Alpes MIRA 2007, 2008 and 2010; Association pour la Recherche sur le Cancer n° [ECL2010R01122, Indo-French program CEFIPRA n° 3803-1]; CNRS; Ecole Normale Supérieure de Lyon. Spanish MINECO [SAF2012-39749 and RYC2010-07337 Toward research in the Buschbeck lab]. A postdoctoral Juan de la Cierva fellowship (to J.D.) and a Ramón Y Cajal fellow (MINECO) (to M.B.). Funding for open access: Ecole Normale Supérieure de Lyon.

Conflict of interest statement. None declared.

REFERENCES

1. Moss,T., Langlois,F., Gagnon-Kugler,T. and Stefanovsky,V. (2007) A housekeeper with power of attorney: the rRNA genes in ribosome biogenesis. *Cell. Mol. Life Sci.*, **64**, 29–49.
2. Henderson,A.S., Warburton,D. and Atwood,K.C. (1972) Location of ribosomal DNA in the human chromosome complement. *Proc. Natl Acad. Sci. USA*, **69**, 3394–3398.
3. McStay,B. and Grummt,I. (2008) The epigenetics of rRNA genes: from molecular to chromosome biology. *Annu. Rev. Cell Dev. Biol.*, **24**, 131–157.
4. Grummt,I. and Langst,G. (2013) Epigenetic control of RNA polymerase I transcription in mammalian cells. *Biochim. Biophys. Acta*, **1829**, 393–404.
5. Santoro,R. (2011) The epigenetics of the nucleolus: Structure and function of active and silent ribosomal RNA genes. In: Olson,M.O.J. (ed.), *The Nucleolus*. Springer, New York, pp. 57–82, Protein Review 15. Series Editor: M Zouhair Atassi.
6. Yuan,X., Feng,W., Imhof,A., Grummt,I. and Zhou,Y. (2007) Activation of RNA polymerase I transcription by cockayne syndrome group B protein and histone methyltransferase G9a. *Mol. Cell*, **27**, 585–595.
7. Gagnon-Kugler,T., Langlois,F., Stefanovsky,V., Lessard,F. and Moss,T. (2009) Loss of human ribosomal gene CpG methylation enhances cryptic RNA polymerase II transcription and disrupts ribosomal RNA processing. *Mol. Cell*, **35**, 414–425.
8. Xie,W., Ling,T., Zhou,Y., Feng,W., Zhu,Q., Stunnenberg,H.G., Grummt,I. and Tao,W. (2012) The chromatin remodeling complex NuRD establishes the poised state of rRNA genes characterized by bivalent histone modifications and altered nucleosome positions. *Proc. Natl Acad. Sci. USA*, **109**, 8161–8166.
9. Cong,R., Das,S., Ugrinova,I., Kumar,S., Mongelard,F., Wong,J. and Bouvet,P. (2012) Interaction of nucleolin with ribosomal RNA genes and its role in RNA polymerase I transcription. *Nucleic Acids Res.*, **40**, 9441–9454.
10. Araya,I., Nardocci,G., Morales,J., Vera,M., Molina,A. and Alvarez,M. (2010) MacroH2A subtypes contribute antagonistically to the transcriptional regulation of the ribosomal cistron during seasonal acclimatization of the carp fish. *Epigenetics Chromatin*, **3**, 14.
11. Posavec,M., Timinszky,G. and Buschbeck,M. (2013) Macro domains as metabolite sensors on chromatin. *Cell. Mol. Life Sci.*, **70**, 1509–1524.
12. Creppe,C., Janich,P., Cantarino,N., Noguera,M., Valero,V., Musulen,E., Douet,J., Posavec,M., Martin-Caballero,J., Sumoy,L. *et al*. (2012) MacroH2A1 regulates the balance between self-renewal and differentiation commitment in embryonic and adult stem cells. *Mol. Cell Biol.*, **32**, 1442–1452.
13. Gamble,M.J., Frizzell,K.M., Yang,C., Krishnakumar,R. and Kraus,W.L. (2010) The histone variant macroH2A1 marks repressed autosomal chromatin, but protects a subset of its target genes from silencing. *Genes Dev.*, **24**, 21–32.
14. Ouararhni,K., Hadj-Slimane,R., Ait-Si-Ali,S., Robin,P., Mietton,F., Harel-Bellan,A., Dimitrov,S. and Hamiche,A. (2006) The histone variant mH2A1.1 interferes with transcription by down-regulating PARP-1 enzymatic activity. *Genes Dev.*, **20**, 3324–3336.
15. Angelov,D., Bondarenko,V.A., Almagro,S., Menoni,H., Mongelard,F., Hans,F., Mietton,F., Studitsky,V.M., Hamiche,A., Dimitrov,S. *et al*. (2006) Nucleolin is a histone chaperone with FACT-like activity and assists remodeling of nucleosomes. *EMBO J.*, **25**, 1669–1679.
16. Ugrinova,I., Monier,K., Ivaldi,C., Thiry,M., Storck,S., Mongelard,F. and Bouvet,P. (2007) Inactivation of nucleolin leads to nucleolar disruption, cell cycle arrest and defects in centrosome duplication. *BMC Mol. Biol.*, **8**, 66.
17. Buschbeck,M., Uribesalgo,I., Wibowo,I., Rue,P., Martin,D., Gutierrez,A., Morey,L., Guigo,R., Lopez-Schier,H. and Di Croce,L. (2009) The histone variant macroH2A is an epigenetic regulator of key developmental genes. *Nat. Struct. Mol. Biol.*, **16**, 1074–1079.
18. Santoro,R. and Grummt,I. (2001) Molecular mechanisms mediating methylation-dependent silencing of ribosomal gene transcription. *Mol. Cell*, **8**, 719–725.
19. Hernandez-Munoz,I., Lund,A.H., van der Stoop,P., Boutsma,E., Muijrers,I., Verhoeven,E., Nusinow,D.A., Panning,B., Marahrens,Y. and van Lohuizen,M. (2005) Stable X chromosome inactivation involves the PRC1 Polycomb complex and requires histone MACROH2A1 and the CULLIN3/SPOP ubiquitin E3 ligase. *Proc. Natl Acad. Sci. USA*, **102**, 7635–7640.
20. Ghoshal,K., Majumder,S., Datta,J., Motiwala,T., Bai,S., Sharma,S.M., Frankel,W. and Jacob,S.T. (2004) Role of human ribosomal RNA (rRNA) promoter methylation and of methyl-CpG-binding protein MBD2 in the suppression of rRNA gene expression. *J. Biol. Chem.*, **279**, 6783–6793.
21. Conconi,A., Widmer,R.M., Koller,T. and Sogo,J.M. (1989) Two different chromatin structures coexist in ribosomal RNA genes throughout the cell cycle. *Cell*, **57**, 753–761.

22. Dammann,R., Lucchini,R., Koller,T. and Sogo,J.M. (1993) Chromatin structures and transcription of rDNA in yeast *Saccharomyces cerevisiae*. *Nucleic Acids Res.*, **21**, 2331–2338.
23. Rickards,B., Flint,S.J., Cole,M.D. and LeRoy,G. (2007) Nucleolin is required for RNA polymerase I transcription *in vivo*. *Mol. Cell. Biol.*, **27**, 937–948.
24. Storck,S., Thiry,M. and Bouvet,P. (2009) Conditional knockout of nucleolin in DT40 cells reveals the functional redundancy of its RNA-binding domains. *Biol. Cell*, **101**, 153–167.
25. Andersen,J.S., Lyon,C.E., Fox,A.H., Leung,A.K., Lam,Y.W., Steen,H., Mann,M. and Lamond,A.I. (2002) Directed proteomic analysis of the human nucleolus. *Curr. Biol.*, **12**, 1–11.
26. Scherl,A., Coute,Y., Deon,C., Calle,A., Kindbeiter,K., Sanchez,J.C., Greco,A., Hochstrasser,D. and Diaz,J.J. (2002) Functional proteomic analysis of human nucleolus. *Mol. Biol. Cell*, **13**, 4100–4109.
27. Gaspar-Maia,A., Qadeer,Z.A., Hasson,D., Ratnakumar,K., Adrian Leu,N., Leroy,G., Liu,S., Costanzi,C., Valle-Garcia,D., Schaniel,C. *et al.* (2013) MacroH2A histone variants act as a barrier upon reprogramming towards pluripotency. *Nat. Commun.*, **4**, 1565.
28. Changolkar,L.N., Costanzi,C., Leu,N.A., Chen,D., McLaughlin,K.J. and Pehrson,J.R. (2007) Developmental changes in histone macroH2A1-mediated gene regulation. *Mol. Cell. Biol.*, **27**, 2758–2764.
29. Boulard,M., Storck,S., Cong,R., Pinto,R., Delage,H. and Bouvet,P. (2010) Histone variant macroH2A1 deletion in mice causes female-specific steatosis. *Epigenetics Chromatin*, **3**, 8.
30. Pasque,V., Gillich,A., Garrett,N. and Gurdon,J.B. (2011) Histone variant macroH2A confers resistance to nuclear reprogramming. *EMBO J.*, **30**, 2373–2387.
31. Mongelard,F. and Bouvet,P. (2007) Nucleolin: a multiFACeTed protein. *Trends Cell Biol.*, **17**, 80–86.
32. Gaume,X., Monier,K., Argoul,F., Mongelard,F. and Bouvet,P. (2011) *In vivo* study of the histone chaperone activity of nucleolin by FRAP. *Biochem. Res. Int.*, **2011**, 187624.
33. Csankovszki,G., Panning,B., Bates,B., Pehrson,J.R. and Jaenisch,R. (1999) Conditional deletion of Xist disrupts histone macroH2A localization but not maintenance of X inactivation. *Nat. Genet.*, **22**, 323–324.
34. Mayer,C., Schmitz,K.M., Li,J., Grummt,I. and Santoro,R. (2006) Intergenic transcripts regulate the epigenetic state of rRNA genes. *Mol. Cell*, **22**, 351–361.
35. Hochstatter,J., Holzel,M., Rohrmoser,M., Schermelleh,L., Leonhardt,H., Keough,R., Gonda,T.J., Imhof,A., Eick,D., Langst,G. *et al.* (2012) Myb-binding protein 1a (Mybbp1a) regulates levels and processing of pre-ribosomal RNA. *J. Biol. Chem.*, **287**, 24365–24377.
36. Stefanovsky,V., Langlois,F., Gagnon-Kugler,T., Rothblum,L.I. and Moss,T. (2006) Growth factor signaling regulates elongation of RNA polymerase I transcription in mammals via UBF phosphorylation and r-chromatin remodeling. *Mol. Cell*, **21**, 629–639.
37. Tolstorukov,M.Y., Goldman,J.A., Gilbert,C., Ogryzko,V., Kingston,R.E. and Park,P.J. (2012) Histone variant H2A.Bbd is associated with active transcription and mRNA processing in human cells. *Mol. Cell*, **47**, 596–607.